Role of Actin Polymerization and Adhesion to Extracellular Matrix in Rac- and Rho-induced Cytoskeletal Reorganization

Laura M. Machesky* and Alan Hall‡

*Department of Molecular Medicine, ‡Department of Biochemistry and Molecular Biology, Medical Research Council Laboratory for Molecular Cell Biology, University College London, London WC1E 6BT, United Kingdom

Abstract. Most animal cells use a combination of actin-myosin–based contraction and actin polymerization–based protrusion to control their shape and motility. The small GTPase Rho triggers the formation of contractile stress fibers and focal adhesion complexes (Ridley, A.J., and A. Hall. 1992. *Cell.* 70:389–399) while a close relative, Rac, induces lamellipodial protrusions and focal complexes in the lamellipodium (Nobes, C.D., and A. Hall. 1995. *Cell.* 81:53–62; Ridley, A.J., H.F. Paterson, C.L. Johnston, D. Diekmann, and A. Hall. 1992. *Cell.* 70:401–410); the Rho family of small GTPases may thus play an important role in regulating cell movement. Here we explore the roles of actin polymerization and extracellular matrix in Rho- and Rac-stimulated cytoskeletal changes. To examine the underlying mechanisms through which these GTPases control F-actin assembly, fluorescently labeled monomeric actin, Cy3-actin, was introduced into serum-starved Swiss 3T3 fibroblasts. Incorporation of Cy3-actin into lamellipodial protrusions is concomitant with F-actin assembly after activation of Rac, but Cy3-actin is not incorporated into stress fibers formed immediately after Rho activation. We conclude that Rac induces rapid actin polymerization in ruffles near the plasma membrane, whereas Rho induces stress fiber assembly primarily by the bundling of actin filaments. Activation of Rho or Rac also leads to the formation of integrin adhesion complexes. Integrin clustering is not required for the Rho-induced assembly of actin-myosin filament bundles, or for vinculin association with actin bundles, but is required for stress fiber formation. Integrin-dependent focal complex assembly is not required for the Rac-induced formation of lamellipodia or membrane ruffles. It appears, therefore, that the assembly of large integrin complexes is not required for most of the actin reorganization or cell morphology changes induced by Rac or Rho activation in Swiss 3T3 fibroblasts.

Movement of most animal cells depends on the coordinated extension of a lamella in the direction of motion (the leading edge) and retraction of the uropod at the rear of the cell. Moving cells show actin-rich leading lamellae in which the actin filaments undergo rapid turnover (31, 32) and more stable actin-myosin cables (acto-myosin) found near the middle and rear of the cell as well as in more established protrusions (7). This has led to the hypothesis that cell motility involves the coordinated polymerization of actin at the leading edge, to push out the membrane, and contraction of actin-myosin cables at the rear. Other factors may also be important for cell motility, such as recycling of the plasma membrane (2, 19) and integrin-mediated adhesion (35).

The Rho family of small GTPases is in an ideal position to control cell motility and morphology in response to extracellular stimuli. Activation of Rho in fibroblasts, for example, results in the assembly of stress fibers and focal adhesions (24), while activation of Rac causes extension of peripheral lamellipodia and assembly of small focal complexes (20, 25). A third member of the Rho GTPase family, Cdc42, regulates the formation of peripheral filopodial extensions (20). In serum-starved Swiss 3T3 mouse fibroblasts, PDGF has been shown to be a potent activator of Rac, whereas lysophosphatidic acid and sphingosine-1-phosphate (sphingosine-1-p)[1] induce stress fiber formation through activation of Rho (22, 24).

One of the molecular events that has been assumed to occur when Rac or Rho is activated is actin polymerization. Actin polymerization is a common response of highly motile cells to chemoattractants (5a, 11, 14), supporting the idea that the ability to polymerize actin in a directional way is important for motility and regulation of cell shape. Neutrophils (5a) and *Dictyostelium* amoebas (11), for example, show an approximate doubling of filamentous actin (F-actin) upon f-Met-Leu-Phe or cAMP stimulation, re-

Please address all correspondence to Laura M. Machesky, Department of Molecular Medicine, Medical Research Council Laboratory for Molecular Cell Biology, University College London, Gower Street, London WC1E 6BT, United Kingdom. Tel.: (44) 171-380-7911. Fax: (44) 171-380-7805. e-mail: dmcblam@ucl.ac.uk

1. *Abbreviations used in this paper*: F-actin, filamentous actin; SFM, serum-free medium; sphingosine-1-p, sphingosine-1-phosphate.

spectively, and this is due, at least in part, to uncapping of actin filaments (5a, 36). It has been proposed that phosphatidylinositol 4,5 bisphosphate (PI 4,5 P_2) can regulate actin polymerization through its ability to bind to several actin-binding proteins and to alter their activities (30). One of the clearest demonstrations of this has been in platelets, where a thrombin-stimulated increase in PI 4,5 P_2 correlates with uncapping of actin filaments (12). Hartwig et al. (12) have been able to mimic the effects of thrombin on PI 4,5 P_2 levels and actin polymerization by adding activated recombinant Rac to permeabilized platelets. Addition of recombinant constitutively active Rho did not cause this effect in permeabilized platelets, although it may also be linked to polyphosphoinositide signaling, as it has been reported to interact with and modulate phosphatidylinositol 4P 5-kinase activity in vitro (6, 23).

Adherence of cells to extracellular matrix mediated through integrins is essential for normal vertebrate development and response to injury and appears to be required for cell movement. Integrins cluster while adhering to extracellular matrix in the presence of growth factors and recruit proteins such as vinculin, talin, and paxillin to form focal adhesion complexes (3, 4). Focal adhesion complexes are thought to be important not only for cell adhesion, but also to provide attachment points through which actin and myosin can generate tension in a similar way that a Z-band in a muscle anchors the acto-myosin fibrils (3–5). Both Rac and Rho induce the clustering of integrins to produce focal complexes and focal adhesions, respectively (20, 24, 25). Focal complexes induced by Rac activation are considerably smaller than focal adhesions induced by Rho and are presumably more dynamic, as they are a part of the highly dynamic lamellipodium, but both structures are to date thought to be composed of the same proteins (vinculin, talin, paxillin, etc.) (20). The role of these Rac-induced complexes is totally unclear.

We show here that Rho and Rac act on different pools of actin to trigger cytoskeletal changes. Rac-induced lamellipodia are generated through localized actin polymerization at the cell periphery, which is independent of integrin complex assembly. Rho-induced stress fibers, on the other hand, are generated by integrin-independent bundling of actin filaments and integrin-dependent reorganization into parallel contractile bundles.

Materials and Methods

Reagents

All reagents were purchased from Sigma Chemical Co. (Poole, UK) unless stated otherwise. Sphingosine-1-p was purchased from Calbiochem (Nottingham, UK). Cy3-dye was purchased from Amersham (Little Chalfont, UK). Rhodamine-labeled nonmuscle actin was purchased from Cytoskeleton (Denver, CO). Antibodies were from the following sources: vinculin monoclonal (Sigma), paxillin monoclonal (Zymed Laboratories, Inc., South San Francisco, CA), talin monoclonal (Sigma) and talin polyclonal (kindly provided by K. Burridge, University of North Carolina, Chapel Hill, NC, to A. Hall), and myosin light chain monoclonal (Sigma). Fluorescein dextran (mol wt 10,000, lysine-fixable) and rhodamine phalloidin were purchased from Molecular Probes, Inc. (Eugene, OR).

Cell Culture

Cell culture reagents were purchased from Nunc (Roskilde, Denmark) unless stated otherwise. Swiss 3T3 fibroblasts were cultured as described previously by seeding at high density onto tissue culture grade plastic (Nunclon) in DME containing 5% FCS, penicillin, and streptomycin (20). Cells were allowed to reach confluence, and 7–10 d after seeding cells were serum starved for 16 h by removal of the medium and replacement with serum-free medium (SFM; DME plus 0.2% $NaHCO_3$).

Extracellular Matrix Experiments

Extracellular matrix experiments were performed as previously described (1, 13) for fibronectin-, Con A–, and poly-L-lysine–coated coverslips. Briefly, acid-washed glass coverslips were coated overnight at 4°C with 50 μg/ml fibronectin or 0.5 mg/ml Con A in PBS (1) or 1 h at room temperature with 10 μg/ml poly-L-lysine. Quiescent serum-starved Swiss 3T3 cells were trypsinized and trypsin was neutralized with 0.5 mg/ml soybean trypsin inhibitor in SFM. Cells were washed in SFM, plated, and allowed to attach to coated coverslips (2 h for fibronectin or 30 min for poly-L-lysine).

Inhibitors and growth factors were added to cells in SFM for times indicated in the text at the following concentrations: PDGF-BB at 5 ng/ml (13), and sphingosine-1-p at 5 μM (22).

Protein Expression, Microinjection, and Immunofluorescence

Recombinant small GTPases were expressed as glutathione-S-transferase fusion proteins, purified with glutathione agarose, and cleaved with thrombin as described previously (25). Cells were microinjected with recombinant proteins as described previously (20). We used L63 Rho and L61 Rac mutants for the constitutively active forms. For time courses of microinjection, cells were injected for 5 min and then placed in fixative immediately (0–5-min time points) or after the indicated incubation at 37°C. GTPases were injected at 0.3–0.5 mg/ml, and Cy3-actin was at 20 μM. We estimate that one-tenth of the volume of the cell was injected for all microinjections (20).

Cells were fixed for 10 min in PBS containing 4% paraformaldehyde, and then free amino groups were blocked with 50 mM NH_4Cl for 10 min. Cells were permeabilized using 0.1% Triton-X 100 in PBS and then incubated with appropriate antibodies or fluorescent phalloidin. Antibodies were diluted in PBS containing 1% FCS, rhodamine or fluorescein phalloidin was diluted in PBS, and incubation times were 20 min in all cases. For vinculin staining, we used a mouse monoclonal (catalog No. V4505; Sigma), followed by fluorescein goat anti–mouse (Jackson ImmunoResearch, Luton, UK) and then fluorescein donkey anti–goat (Jackson ImmunoResearch, Luton, UK) antibodies. Coverslips were washed three times between all antibody incubations by dipping into PBS.

Measurement of Filamentous Actin Content of Swiss 3T3 Cells

Filamentous actin content of Swiss 3T3 cells was measured using a modification of the method of Howard and Wang (15). Swiss 3T3 cells were cultured to confluence and quiescence in 100-cm dishes containing a glass coverslip to be used as a monitor of cell morphology. After 16 h of serum starvation, the indicated treatment (PDGF, sphingosine-1-p, or serum) was performed at 37°C. After treatment, the coverslip was removed from each dish and fixed for fluorescence microscopy. These were stained with rhodamine phalloidin and observed in the microscope to determine the quality of the response of each dish of cells to treatment. Cells in plates were then washed two times in PBS, and two successive aliquots of 200 μl fixative containing a saturating amount of rhodamine phalloidin were added (20 mM KPO_4, 10 mM Pipes, 5 mM EGTA, 2 mM $MgCl_2$, 0.1% Triton X-100, 3.7% formaldehyde, 2 μM rhodamine phalloidin). Cells were scraped off the plate after each aliquot of fix/stain, transferred to a 1.5-ml tube, and incubated for 1 h at room temperature on a rotator. Cells were pelleted for 2 min in a microfuge, and the pellets were washed in 0.1% saponin, 20 mM KPO_4, 10 mM Pipes, 5 mM EGTA, 2 mM $MgCl_2$. Pellets were then resuspended in methanol to extract the rhodamine phalloidin and incubated for 1 h on a rotator at room temperature. Rhodamine phalloidin binding was measured for each sample with the fluorescence emission at 563 nm and excitation at 542 nm. Filamentous actin content was expressed as a comparison with values obtained for untreated cells processed in parallel on the same day. Each time point consists of six independent dishes of cells, except the sphingosine-1-p experiments which were repeated 12 times. We confirmed that approximately the same number of cells was used in each time point with the bicinchoninic acid protein

assay (Pierce Chemical Co., Rockford, IL) by measuring the protein concentration in the supernatant of the lysis step. We found this measurement to be linearly related to cell number in the range used for these experiments (data not shown).

Data analysis for F-actin quantitation was carried out using the program Microsoft Excel 5.0™ for the two-tailed *t* test assuming unequal variance among the samples. Confidence levels (obtained by the *t* test) that each experimental mean is different from the equivalent control value (starved cells) are discussed in the legend to Fig. 1, expressed as percentage of confidence. We also quantitated the percentage of cells responding to each treatment by counting cells under the microscope.

Cy3-actin Preparation and Characterization

Approximately 100 mg of rabbit muscle actin was purified from 5 g muscle acetone powder prepared according to Spudich and Watt (29). After the final centrifugation step of the actin preparation, the top two-thirds of the actin was taken from the centrifuge tube, to avoid the pellet or larger oligomers, and dialyzed into labeling and polymerization buffer (0.1 M sodium carbonate, pH 9, 0.1 M KCl, 2 mM $MgCl_2$, 0.3 mM ATP, 0.5 mM DTT) for 24 h against three times 500 ml. Alternatively, we gel filtered the actin at this stage on an S-300 column before dialyzing into labeling buffer (21). A 1.4-ml aliquot of the polymerized actin at 5 mg/ml was added to a tube of reactive Cy3 *N*-hydroxysuccinimide for 30 min at room temperature. This mixture was then dialyzed for 2 d against three times 500 ml buffer G (2 mM Tris-Cl, pH 7.5, 0.2 mM ATP, 0.5 mM DTT, 2 mM $CaCl_2$) to remove unbound dye and to depolymerize the actin. The labeled actin was centrifuged for 30 min at 120,000 *g* to remove polymer, and the top two-thirds of each tube was frozen in liquid N_2 and stored at −70°C for use in microinjection experiments. The ratio of dye to actin monomer was calculated for each preparation by comparing the absorbance at 290 nm (extinction coefficient of 38.5 μM/OD for actin) to the absorbance at 344 nm according to the manufacturer's instructions. Cy3 labeling was directly visualized by running the monomeric actin on SDS-PAGE and viewing a single fluorescent band at ~43 kD with UV light (not shown).

Because Cy3-actin has not to our knowledge been described in the literature before, we characterized it to ensure that it is a suitable probe for actin dynamics in live cells. By comparison of the protein concentration with the absorbance at 344 nm, we estimate that our preparations contained on average one molecule of Cy3-dye per 1.6 actin monomers and in no cases more than one Cy3 per actin monomer. To confirm that Cy3-actin was capable of polymerization, a 3 μM solution of Cy3-actin in buffer G was polymerized by addition of 0.1 vol 10× KME salts (500 mM KCl, 20 mM $MgCl_2$, 1 mM EGTA) and monitoring polymer formation by light scattering at 90° in a fluorometer (Shimadzu Scientific Instruments, Inc., Columbia, MD) as previously described (34). Cy3-actin polymerized somewhat faster than nonlabeled actin, indicating the presence of some oligomers in the preparation (data not shown). This is unlikely to be significant, as microinjection of oligomers does not detectably alter actin polymerization in cells (27). Previous reports using rhodamine-labeled rabbit muscle actin showed that all F-actin–containing cellular structures in fibroblasts could incorporate monomeric muscle actin (33). For most of our experiments we used non–gel-filtered actin, but gel-filtered Cy3-actin behaved identically in cells (data not shown).

Monomeric Cy3-labeled actin was microinjected into Swiss 3T3 fibroblasts growing in 10% serum. Within 5 min of injection, and up to 15 min after injection, Cy3-actin is concentrated in ruffling lamellipodia and not in stress fibers or other actin bundles in the cell body (data not shown). 20–25 min after injection, Cy3-actin becomes incorporated into stress fibers and actin bundles and, by 40 min, all structures that are labeled with fluorescein phalloidin contain Cy3-actin (data not shown). This time course agrees roughly with other studies that used rhodamine-labeled actin (7, 32, 33) and suggests that the ruffling lamellipodium is an area of high actin filament turnover and polymerization of monomeric actin, while the F-actin filaments in stress fibers turn over slowly, with an estimated half-life of 20 min. Nonmuscle actin labeled with rhodamine or gel-filtered muscle actin labeled with Cy3 yielded a similar time course of incorporation first into ruffling lamellipodia and then into stress fibers (data not shown).

Quantitation of Cy3-actin Concentrated in the Lamellipodia of PDGF-treated and Constitutively Activated Rac-injected Cells

We coinjected serum-starved confluent quiescent Swiss 3T3 cells with 4 mg/ml fluorescein dextran and 20 μM Cy3-actin with or without constitutively active recombinant Rac. We used a cooled CCD camera (C4880; Hamamatsu Phototonics, Bridgewater, NJ) to photograph injected cells in both the fluorescein and rhodamine channels. We compared the intensity of the cell body with the intensity in the lamellipodium for both dextran (as a control for cell thickness) and Cy3-actin. The ratio of cell body to lamellar intensity was compared for dextran and Cy3-actin to obtain an estimate of how much Cy3-actin was concentrated in the lamellipodium as a result of factors other than cell thickness and diffusion. We did not observe any bleed-through fluorescence of fluorescein dextran or Cy3-actin under the conditions used for this study. Data analysis was carried out using the program Microsoft Excel 5.0™ for the *t* test assuming unequal variance among the samples. Confidence levels that the experimental mean is different from the value obtained for the starved cells are expressed as a percentage of confidence in the legend to Fig. 5.

Results

Quantitation of Total F-actin in Swiss 3T3 Cells during Lamellipodium and Stress Fiber Formation

Serum starvation of confluent quiescent Swiss 3T3 cells causes the loss of stress fibers, actin-rich lamellipodia, and membrane ruffles (24, 25). Using a modified version of the rhodamine phalloidin binding assay of Howard and Wang (15), we found that serum starvation for 18 h also reduced the F-actin content of cells by ~50% (data not shown).

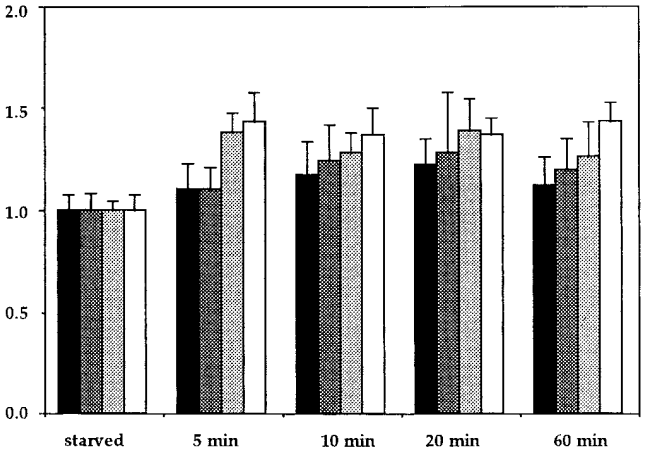

Figure 1. Quantitation of F-actin in cells responding to various stimuli. Bar graphs show the quantity of filamentous actin relative to serum-starved cells (defined as 1). Samples were taken at 5, 10, 20, and 60 min after addition of the stimulus and processed as described in Materials and Methods. (*Black bars*) Sphingosine-1-p treatment; (*dark shaded bars*) PDGF treatment; (*light shaded bars*) sphingosine-1-p + PDGF treatment; (*white bars*) serum treatment. F-actin was calculated by measuring fluorescence of extracted rhodamine phalloidin in a fluorometer as described. Error bars represent the standard deviation from at least six separate experiments per time point. Statistical analysis of the data using the *t* test with unequal variance showed means (μ) and confidence (expressed as percentage) as follows. Sphingosine-1-p: 5 min, μ = 1.10 (97%), 10 min, μ = 1.17 (>99%), 20 min, μ = 1.22 (>99%), 60 min, μ = 1.12 (98%); PDGF: 5 min, μ = 1.11 (92%), 10 min, μ = 1.24 (98%), 20 min, μ = 1.28 (94%), 60 min, μ = 1.20 (98%); sphingosine-1-p plus PDGF: 5 min, μ = 1.38 (>99%), 10 min, μ = 1.28 (>99%), 20 min, μ = 1.39 (99%), 60 min, μ = 1.26 (97%); serum: 5 min, μ = 1.43 (>99%), 10 min, μ = 1.37 (>99%), 20 min, μ = 1.37 (>99%), 60 min, μ = 1.43 (>99%). Confidence levels represent the confidence that each mean experimental value is different from the equivalent mean value for the control (starved cells) using the *t* test.

This depolymerization could provide a pool of actin monomer in starved cells so that a burst of actin polymerization might occur when cells are induced to form stress fibers and/or lamellipodia by activation of Rac or Rho. We measured F-actin levels in cells before and after stimulation with sphingosine-1-p to activate Rho, PDGF to activate Rac, sphingosine-1-p plus PDGF to activate both Rac and Rho, or serum to simulate a return to normal growing conditions. All treatments increased the F-actin levels somewhat (Fig. 1). Sphingosine-1-p addition (Fig. 1, *black bars*) caused a transient rise to 22% above resting levels of F-actin, which had decreased to 12% above background by 60 min. PDGF addition (Fig. 1, *dark shaded bars*) caused a somewhat larger and more sustained response to a maximum of 28% above baseline, which decreased back to 20% by 60 min. Within 5 min of addition, sphingosine-1-p plus PDGF (Fig. 1, *light shaded bars*) or serum (Fig. 1, *white bars*) completely restored F-actin levels to near prestarvation values and sustained this increased level for 60 min.

All treatments resulted in most of the cells responding appropriately (stress fibers or ruffles or some combination). Treatment of cells with sphingosine-1-p or serum resulted in stress fiber formation in 100% of the cells over the time course, whereas ruffling was more variable, and more difficult to quantify, as sizes of lamellipodia varied widely. At least 500 cells were counted for each point. Representative cells from each time point are shown in Fig. 2. Fig. 2 *a* shows starved cells, which do not contain stress fibers, and <5% of the cells show any ruffles. Within 5 min of PDGF addition, 93% of cells show extensive ruffling (not shown), which is sustained for at least 20 min (91% at 10 min, 89% at 20 min; Fig. 2 *b*). By 60 min, only 16% of cells are ruffling (Fig. 2 *c*). This shows a rough correlation with the time course of the changes in F-actin levels in response to PDGF shown in Fig. 1, although the decrease in ruffling is clearly more dramatic than the F-actin change. In the first 5 min of sphingosine-1-p addition, 100% of cells show a loose bundling of actin filaments

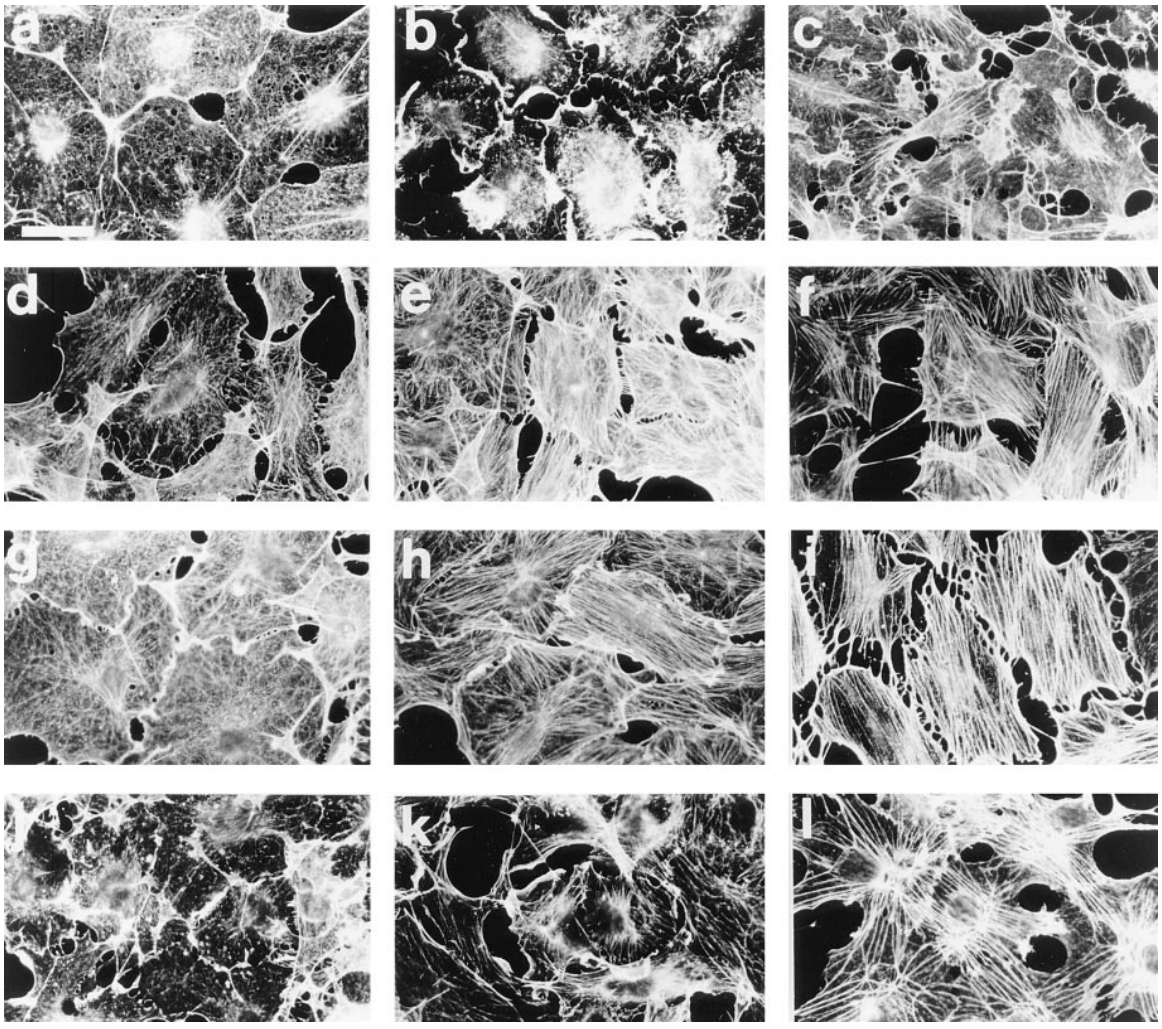

Figure 2. Examples of the cellular response to stimuli used in the quantitation of F-actin experiments. All photos show rhodamine phalloidin labeling of Swiss 3T3 cells taken directly from the F-actin quantitation of Fig. 1. (*a*) Typical serum-starved Swiss 3T3 cells, which are devoid of stress fibers or ruffles. (*b* and *c*) Cells after 20 and 60 min of PDGF stimulation, respectively. (*d–f*) 5, 20, and 60 min, respectively, after stimulation with sphingosine-1-p. (*g–i*) 5, 20, and 60 min, respectively, after addition of 10% serum. (*j–l*) 5, 20, and 60 min after addition of a mixture of both PDGF and sphingosine-1-p. Bar, 10 μm.

(Fig. 2 *d*), which thicken and become straighter during a 60-min time course (Fig. 2, *e* and *f*); fewer than 3% of cells showed any ruffles. Addition of 10% serum to starved cells results in a sustained increase in the proportion of cells ruffling. At 5 min after addition of serum, 44% of the cells are ruffling (Fig. 2 *g*). By 10 min, 82% are ruffling, and at 20 min, 87% of the cells are still ruffling (Fig. 2 *h*). By 60 min 77% of the cells continue to show ruffling (Fig. 2 *i*). In addition to ruffling, 100% of the cells exposed to 10% serum form stress fibers with approximately the same time course as we observed after sphingosine-1-p addition. Addition of both sphingosine-1-p and PDGF to cells largely mimics the addition of serum, with all cells forming stress fibers and a transient increase in the proportion of cells ruffling (5 min, 51%, 10 min, 59%, 20 min, 32%, and 60 min, 18%; Fig. 2, *j*, *k*, and *l*, respectively).

Actin Dynamics Are Affected by the Activation State of Small GTPases

The incorporation of Cy3-actin into F-actin–containing structures in growing cells is likely to be at least partially

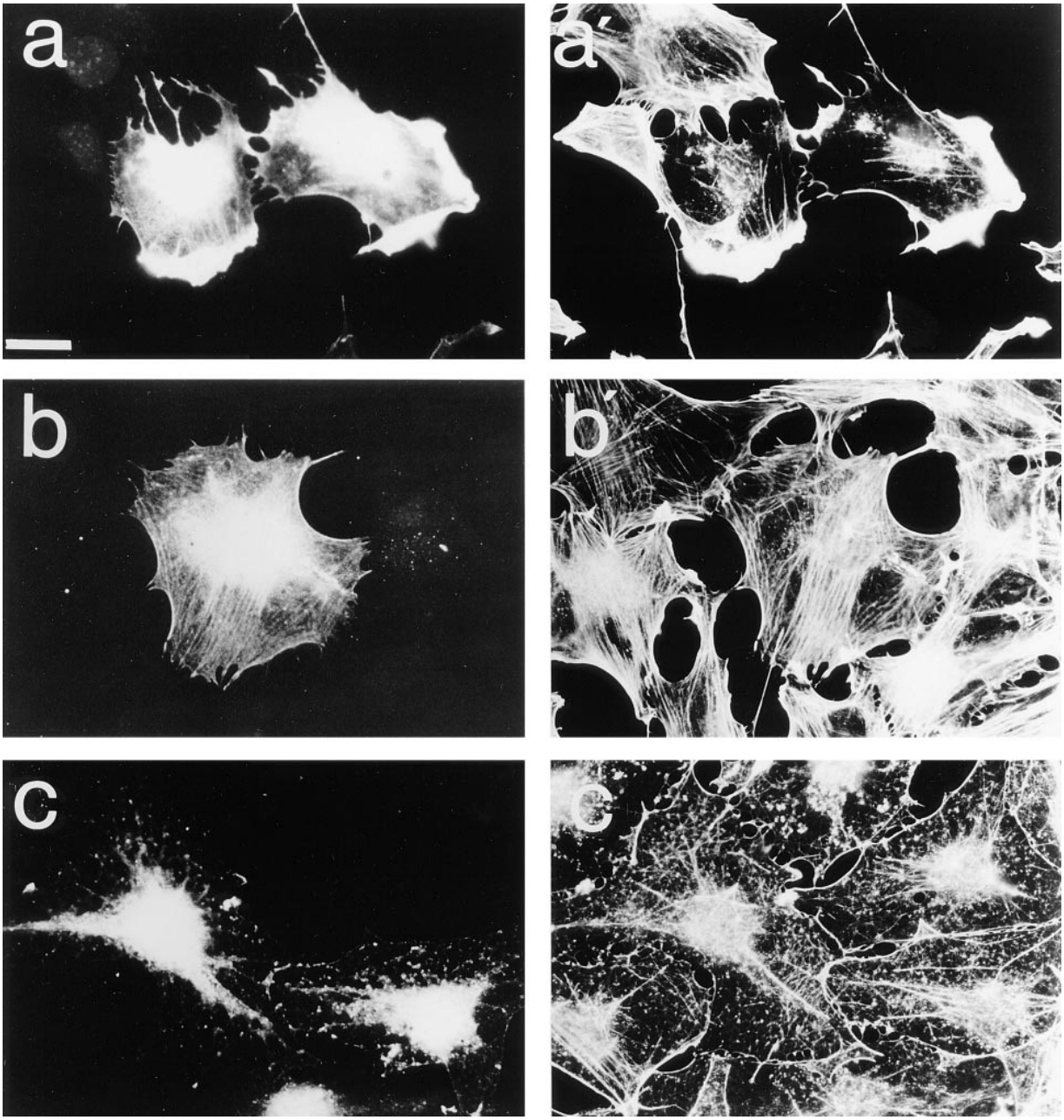

Figure 3. Cy3-actin polymerization is influenced by Rac and Rho activation states. Swiss 3T3 cells growing in 10% serum (*a*, *a′*, *b*, and *b′*) or serum starved overnight (*c* and *c′*) were microinjected with Cy3-actin and inhibitors of Rho (C3-transferase; *a* and *a′*) or Rac (recombinant dominant negative Rac protein; *b* and *b′*). At 20 min after injection, cells were fixed, Cy3-actin was visualized directly (*a*–*c*), and fluorescein phalloidin costaining was used (*a′*–*c′*) to show total F-actin. Bar, 5 μm.

due to the activation state of the small GTPases Rac and Rho. Comicroinjection of Cy3-actin and C3 transferase (to inactivate Rho) had no effect on incorporation of Cy3-actin into lamellipodia even though stress fibers were largely disassembled in these cells after 20 min (Fig. 3, *a* and *a′*). Similarly, coinjection of dominant negative Rac protein with Cy3-actin, which blocked lamellipodia extension and peripheral Cy3-actin incorporation, did not affect the slow rate of incorporation of Cy3-actin into stress fibers (Fig. 3, *b* and *b′*). In serum-starved cells, Cy3-actin remained largely diffuse in the cell body for at least 20 min (Fig. 3, *c* and *c′*). This suggests that Rac and Rho exert separate controls on actin dynamics in the cell, and that in serum-starved conditions, when Rac and Rho have low activity, minimal localized actin polymerization or turnover occurs.

Actin Polymerization in Rac and PDGF-induced Lamellipodia

To determine whether actin polymerization is induced by Rac in Swiss 3T3 cells, recombinant constitutively active Rac protein and Cy3-actin monomer were coinjected into serum-starved Swiss 3T3 cells. Within 5 min of injection, polymerization of Cy3-actin could be observed in the periphery of injected cells (Fig. 4, *a* [Cy3-actin] and *a′* [fluorescein phalloidin counterstain]). The F-actin–containing lamellipodium expanded in injected cells and, by 20–25 min, large ruffling lamellipodia were present that contained Cy3-actin (Fig. 4, *b* [Cy3-actin] and *b′* [fluorescein phalloidin counterstain]).

Cy3-actin also rapidly incorporated into ruffling lamellipodia when starved cells were first injected with Cy3-actin and then treated with PDGF. Within 5 min of PDGF treatment, lamellipodia contained concentrated Cy3-actin (Fig. 4, *c* [Cy3-actin] and *c′* [fluorescein phalloidin counterstain]). At 20–25 min, lamellipodia showed similar localization of Cy3-actin as with recombinant Rac injection (Fig. 4, *d* [Cy3-actin] and *d′* [fluorescein phalloidin counterstain]).

To determine quantitatively whether PDGF addition had essentially the same effect as microinjection of recombinant active Rac, we compared the amount of Cy3-actin incorporated into lamellipodia produced by each treatment. To do this, we photographed at least 20 cells coinjected with a mixture of Cy3-actin, fluorescein dextran, and, for the Rac experiments, constitutively active Rac protein. We compared the intensity of Cy3-actin fluorescence with the level of dextran fluorescence in the lamellipodium to obtain an estimate of how much Cy3-actin had polymerized in the lamellipodium (above levels that would be expected because of cell thickness in this region). An example of the data we obtained is shown in Fig. 5. In each graph (*a–d*) the fluorescence intensity profile of either Cy3-actin or fluorescein dextran is shown as a function of distance across the cell. Cells treated with PDGF (not shown) or injected with Rac (Fig. 5, *c* and *d*) showed relatively larger peripheral fluorescence peaks of Cy3-actin than did starved cells (Fig. 5, *a* and *b*). The ratios of fluorescence intensities are shown in Fig. 5 *e.* Both endogenous and recombinant Rac show identical time courses of activation, with Cy3-actin becoming concentrated in the lamellipodium by 5 min of injection or PDGF treatment. The amount of Cy3-actin accumulation after PDGF treatment was smaller than that after microinjected active Rac (twofold for Rac, Fig. 5 *e*, *white bars*; 1.5-fold for PDGF, Fig. 5 *e*, *gray bars*) and stayed largely constant for both treatments over a time course of 5–20 min. Starved cells showed little or no concentration of Cy3-actin in the periphery (Fig. 5 *e*, *black bars*). We also summed the intensities of all Cy3-actin peaks obtained after either Rac injection or PDGF treatment and found no significant size differences over time with the different treatments (data not shown). Thus, both activation of endogenous Rac by PDGF treatment and microinjection of recombinant activated Rac produce a rapid polymerization and accumulation of actin in peripheral lamellipodia. In addition, since the total intensity of the Cy3-actin fluorescence in the lamellipodium does not increase over the time course, turnover of F-actin must also be similar in the two treatments.

Localized Actin Polymerization Does Not Accompany Rho-induced Stress Fiber Formation

To understand how actin is assembled into stress fibers, we used confocal imaging of de novo stress fiber formation at different times after activation of Rho with sphingosine-1-p. Starved cells contain diffuse and punctate phalloidin staining, as well as actin filament bundles loosely organized on the bottom surface of the cell and around the nucleus. They also typically contain a thick peripheral bundle of actin filaments and sometimes rings of actin filaments that are distributed throughout the cell, primarily on the basal surface (Fig. 6 *a*, *arrow* and *inset*). These structures appear to be bundled actin filaments, which stain with myosin-II antibodies and incorporate Cy3-actin with a half-time of ~20 min (not shown). Electron microscope studies of whole mount preparations of starved cells have shown that the rings are not separate structures, but sites of tight coiling of curvilinear actin bundles (Rottner, K., and J.V. Small, personal communication). By 5 min after sphingosine-1-p addition, most cells show increased aggregation of actin filament bundles (Fig. 6 *b*). These cells also show diffuse phalloidin staining suggestive of nonbundled actin filaments that are below the resolution of the light microscope. By 20 min, parallel arrays of stress fibers (Fig. 6 *c*) (with focal adhesions; not shown) appear in most cells, and these thicken and lengthen by 60 min of treatment (Fig. 6 *d*).

We next examined incorporation of monomeric Cy3-actin into stress fibers after activation of Rho. After addition of sphingosine-1-p for 5 min to confluent quiescent cells, actin bundles are present (Fig. 7 *a′*) even though these are relatively thinner than later stress fibers and poorly organized. They are not detectably labeled with Cy3-actin (Fig. 7 *a*). By 20 min after sphingosine-1-p treatment, some incorporation of Cy3-actin into stress fibers occurs (Fig. 7, *b* and *b′*). At 40 min after treatment, most of the Cy3-actin incorporates into the stress fibers in most cells (Fig. 7, *c* and *c′*). Coinjection of dominant active Rho protein into cells also causes stress fibers to form, which are initially unlabeled with Cy3-actin (10 min after injection; Fig. 7, *d* and *d′*) but gradually incorporate the labeled actin as turnover occurs (20 min after injection; Fig. 7, *e* and *e′*), with nearly complete incorporation by 40 min (not shown).

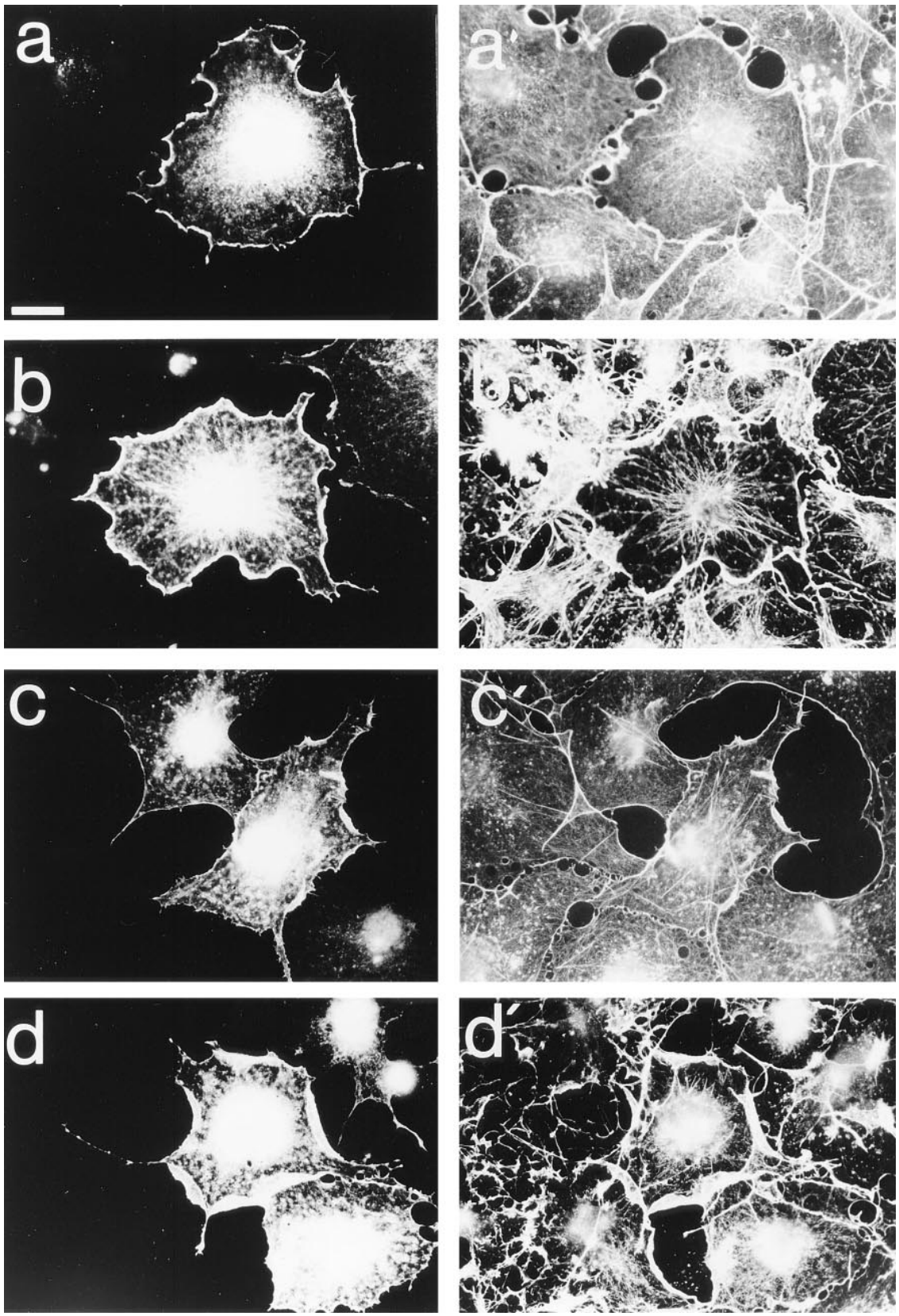

Figure 4. Incorporation of Cy3-actin into ruffling lamellipodia induced by activation of Rac. Serum-starved confluent quiescent Swiss 3T3 cells were microinjected with Cy3-actin and constitutively active Rac protein (*a*, *a′*, *b*, and *b′*) or treated with PDGF (*c*, *c′*, *d*, and *d′*). At 5 min (*a*, *a′*, *c*, and *c′*) or 20 min (*b*, *b′*, *d*, and *d′*) cells were fixed and costained with fluorescein phaloidin to visualize total F-actin. (*a–d*) Cy3-actin; (*a′–d′*) fluorescein phalloidin costain of total F-actin. Bar, 5 μm.

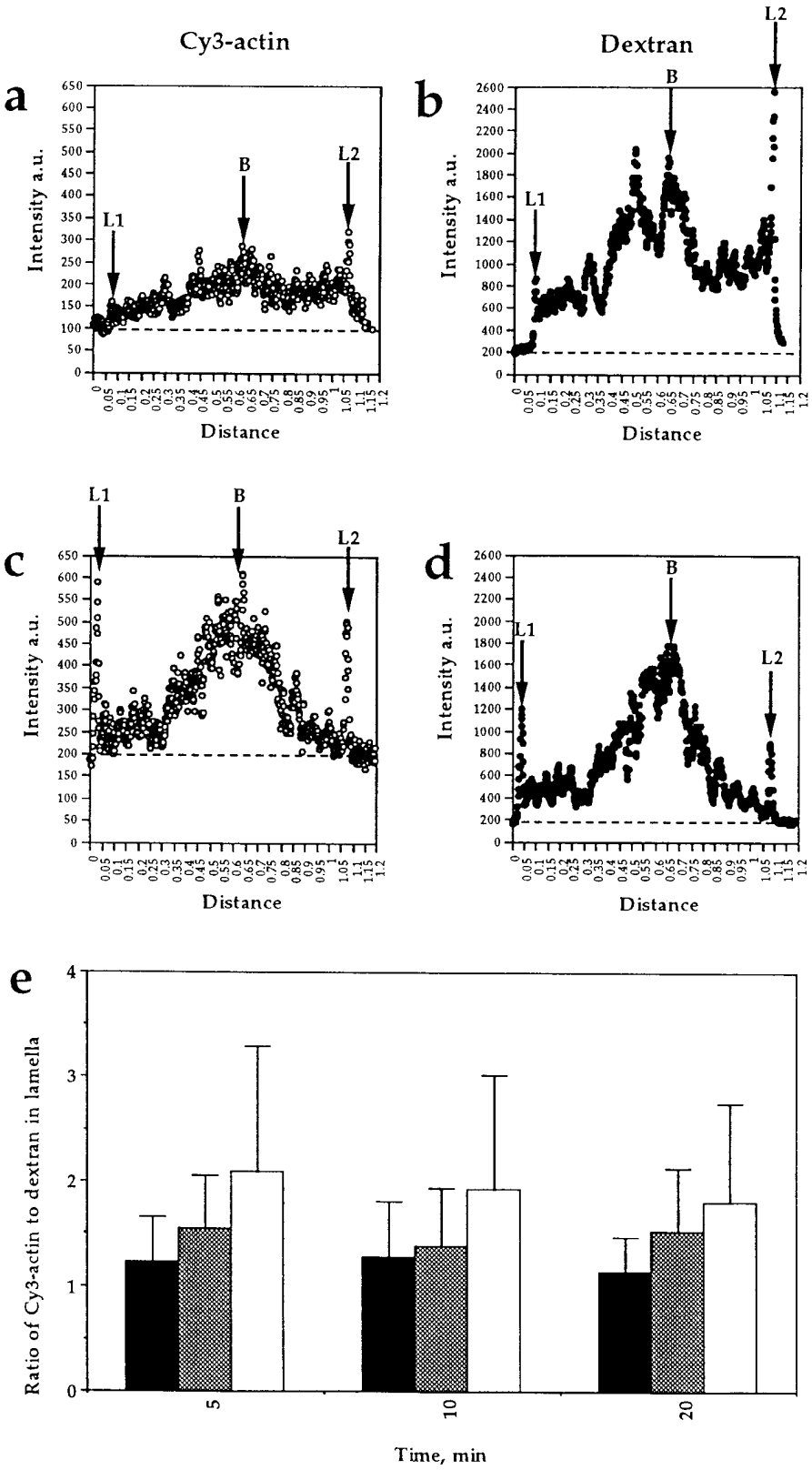

Figure 5. Quantitation of Cy3-actin in Rac or PDGF-induced lamellipodia. Serum-starved quiescent confluent Swiss 3T3 cells were treated under three different conditions: (*a*) injected with fluorescein dextran and Cy3-actin and incubated for 5, 10, or 20 min; (*b*) injected with fluorescein dextran and Cy3-actin and incubated for 5, 10, or 20 min in the presence of PDGF; and (*c*) injected with fluorescein dextran, constitutively active recombinant Rac protein, and Cy3-actin and incubated for 5, 10, or 20 min. The relative amount of Cy3-actin to fluorescein dextran concentrated in the lamellipodium of each cell was quantitated using a Hamamatsu C4880 cooled CCD camera. The fluorescence intensity profiles (for both the red and green fluorescence channels) of a line drawn across an entire starved cell 20 min after Cy3-actin and fluorescein dextran are shown in *a* and *b*. Intensity is in arbitrary units vs distance across the cell in arbitrary units, with ~0.1 U = 5 μm. Similar profiles are shown in *c* and *d* for a starved cell 20 min after injection with constitutively active Rac, Cy3-actin, and fluorescein dextran. The peripheral lamellipodium was defined as the first (*L1*) or last (*L2*) peak of either dextran or actin fluorescence (see *arrows* in *a–d*). The wide peak in the middle of the cell is the cell body near the nucleus (*B*). Dashed lines in each graph indicate the background fluorescence of the substrate, which was subtracted from all peak heights. The bar graph in *e* shows a summary of the relative amount of Cy3-actin (to fluorescein dextran) concentrated in the lamellipodium averaged for at least 20 cells at each condition and time. (*Black bars*) Starved cells injected with Cy3-actin and fluorescein dextran. (*Gray bars*) Starved cells injected with Cy3-actin and fluorescein dextran and treated with PDGF. (*White bars*) Starved cells injected with Cy3-actin, fluorescein dextran, and constitutively active Rac protein. All values obtained for Rac-induced accumulation of Cy3-actin were significantly different from the mean values for the starved cells to >99.5% confidence using the *t* test assuming unequal variance among the samples. For the PDGF-treated cells, the data at 5 min were significantly different from the starved cells with 97% confidence, the data at 10 min were significantly different with 77% confidence, and the data at 20 min were significantly different with 99% confidence.

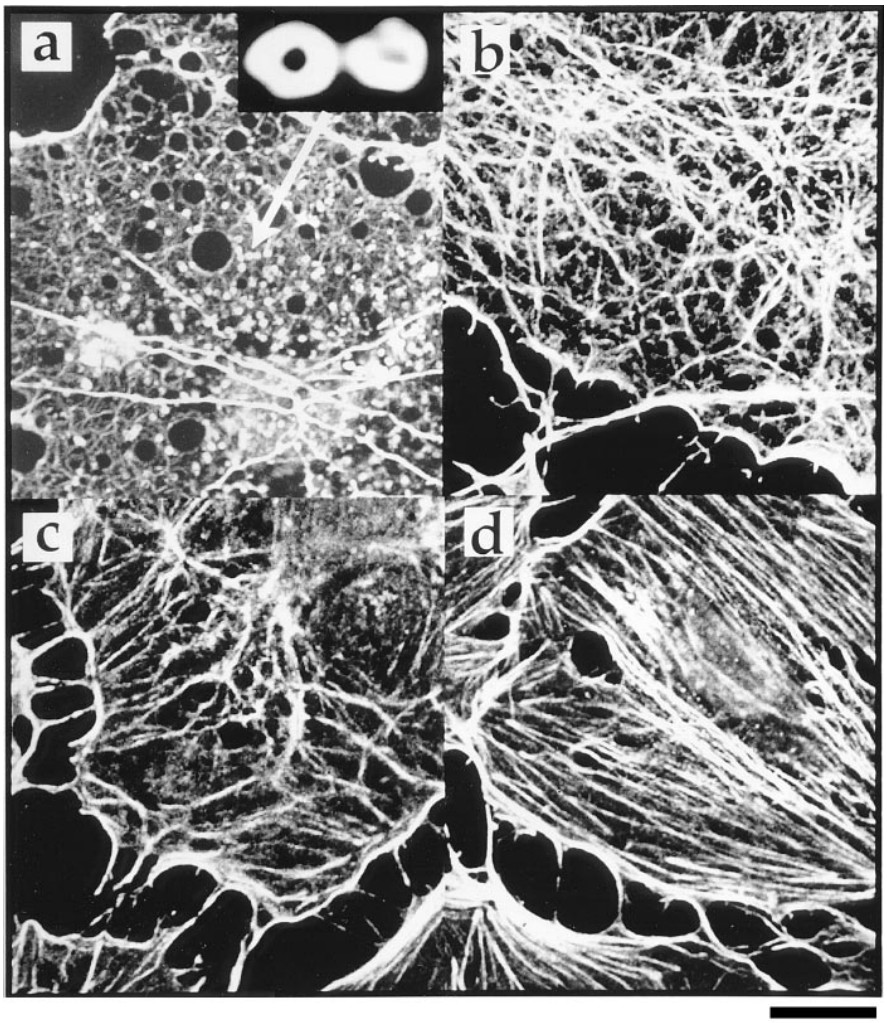

Figure 6. Time course of formation of stress fibers upon Rho activation with sphingosine-1-p. Serum-starved confluent quiescent Swiss 3T3 cells were examined by confocal microscopy to determine the organization of filamentous actin stained with rhodamine phalloidin (*a–d*). (*a*) Filamentous actin in starved cells; arrow in *a* points to rings of filamentous actin seen only in starved cells. (*Inset*) Two rings enlarged an additional 20 times. (*b*) Filamentous actin at 5 min after sphingosine-1-p addition. (*c*) Filamentous actin at 20 min after sphingosine-1-p addition. (*d*) Filamentous actin at 60 min after addition of sphingosine-1-p. Bar, 5 μm.

Role of Extracellular Matrix in Rho-induced Assembly of Stress Fibers and Focal Adhesions

When serum-starved cells are trypsinized and replated on poly-L-lysine, they do not form focal adhesions or stress fibers (13). Fig. 8, *a* and *b*, shows, however, that addition of sphingosine-1-p to cells plated on poly-L-lysine induces a dramatic reorganization of filamentous actin; after stimulation, the periphery of cells is nearly devoid of phalloidin label and the actin is assembled into disorganized bundles in the cell body. Myosin also moves from diffuse cytoplasmic and cortical labeling to colocalize with the actin bundles in the body of the cell (Fig. 8, *c* and *d*). Coinjected Cy3-actin only gradually incorporates into these actin bundles, with a half-time of ~20 min (data not shown), similar to incorporation rates for stress fibers. Interestingly, vinculin can be found concentrated along the length of these actin-myosin cables (Fig. 8, *e* and *f*), but there are no focal adhesion plaques, as there is no extracellular matrix in these conditions. There is also no visible recruitment of talin to these structures (Fig. 8, *g* and *h*) and very little (if any) concentration of paxillin (not shown). In contrast, Rho activation in cells plated on fibronectin causes the assembly of parallel actin stress fibers with both talin and paxillin concentrated in focal adhesions (visualized with the same antibodies; data not shown). Actin-myosin assemblies formed upon Rho activation in cells plated on poly-L-lysine do appear to exert tension, as cells show dramatic rounding, e.g., when sphingosine-1-p is added to cells, as observed under time-lapse video microscopy (data not shown).

To rule out that the accumulation of vinculin along Rho-induced actin bundles in cells on poly-L-lysine was due to small or transient integrin clustering, we used EDTA treatment concomitantly with sphingosine-1-p addition to dissociate integrin complexes. We found that the number of cells containing vinculin clusters formed by Rho activation on poly-L-lysine, and the morphology of these clusters was completely resistant to 1 mM or 10 mM EDTA treatment, whereas 100% of the cells on fibronectin rounded up and lost focal adhesions under these conditions (data not shown).

Role of Extracellular Matrix in Rac-induced Lamellipodium Extension

To determine whether integrin-mediated adhesion is required for the extension of lamellipodia and ruffles, Rac and Cy3-actin were coinjected into cells plated on poly-L-lysine (Fig. 9, *a* and *b*), or PDGF was used to activate endoge-

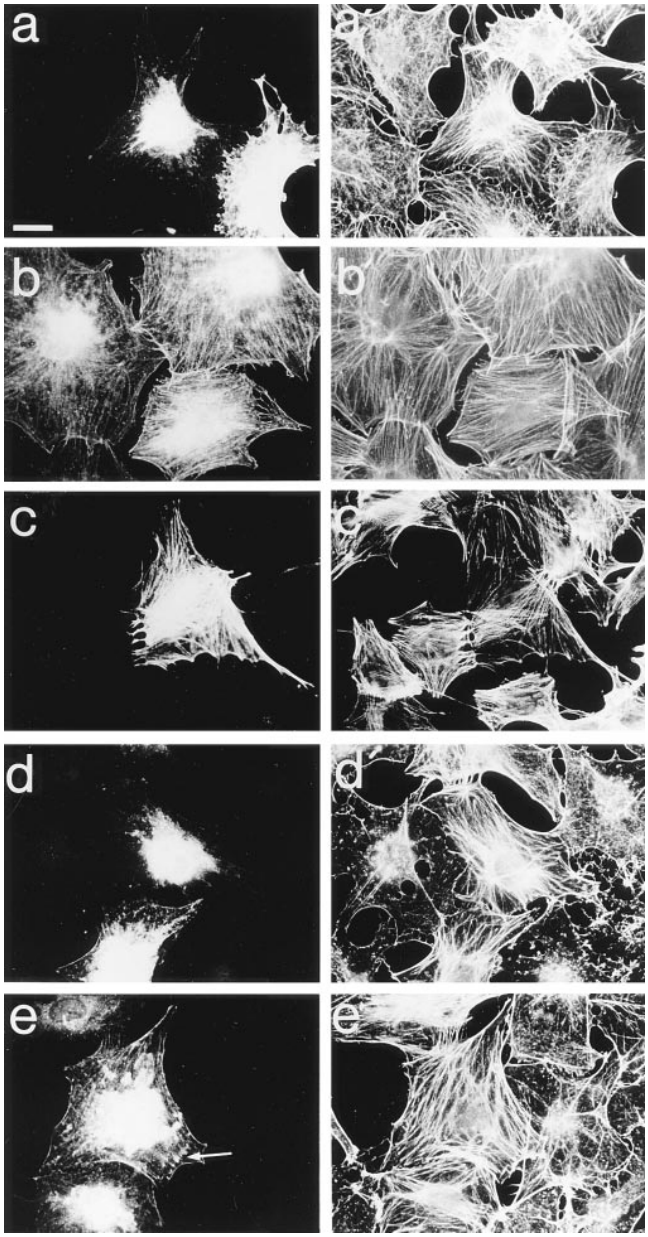

Figure 7. Time course of incorporation of Cy3-actin into stress fibers induced by Rho activation. Serum-starved confluent quiescent Swiss 3T3 cells were treated in two ways to cause Rho activation: either injection of Cy3-actin and then addition of sphingosine-1-p (*a*, *a′*, *b*, *b′*, *c*, and *c′*), or coinjection of Cy3-actin with dominant active Rho protein (*d*, *d′*, *e*, and *e′*). Cells were counterstained with fluorescein phalloidin (*a′–e′*) to compare total filamentous actin to injected Cy3-actin (*a–e*). (*a* and *a′*) Cells injected for 5 min with Cy3-actin and then treated for 5 min with sphingosine-1-p; (*b* and *b′*) Cells injected for 5 min with Cy3-actin and then treated for 20 min with sphingosine-1-p; (*c* and *c′*) Cells injected for 5 min with Cy3-actin and then treated for 40 min with sphingosine-1-p; (*d* and *d′*) Cells injected with Rho protein and Cy3-actin for 5 min and then incubated for 10 min; (*d* and *d′*) Cells injected with Rho protein and Cy3-actin for 5 min and then incubated for 20 min. Bar, 5 μm.

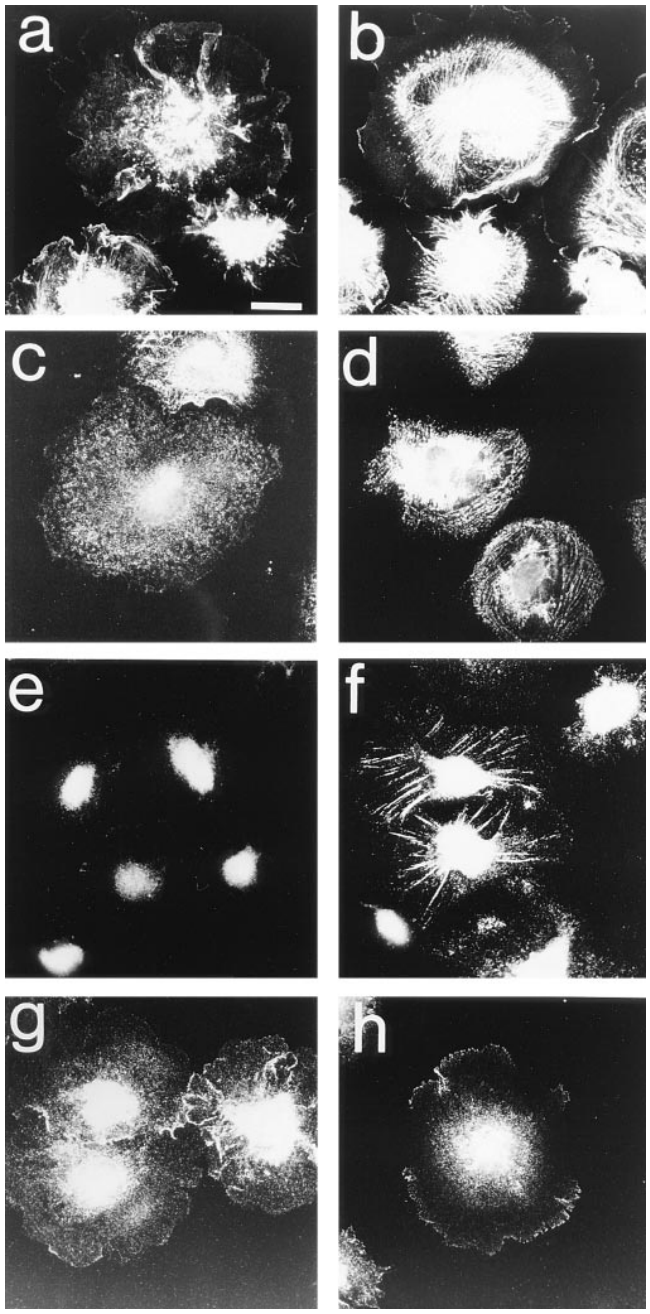

Figure 8. Response of cells plated on poly-L-lysine to Rho activation. Serum-starved quiescent Swiss 3T3 cells were trypsinized and plated onto poly-L-lysine (10 μg/ml)–coated coverslips for 20 min before addition of sphingosine-1-p for 20 min (*b*, *d*, *f*, and *h*) or mock treatment with serum-free medium for 20 min (*a*, *c*, *e*, and *g*). Cells were then fixed and stained for filamentous actin (*a* and *b*), myosin-II light chain (*c* and *d*), vinculin (*e* and *f*), or talin (*g* and *h*). Bar, 5 μm.

nous Rac in cells plated on poly-L-lysine (Fig. 9, *c* and *d*) or Con A (not shown), two substrates that do not lead to integrin clustering. Within 5 min (not shown) and for up to 20 min (Fig. 9 *a*), Cy3-actin accumulated in the expanding lamellipodium of cells plated on poly-L-lysine and colocalized with F-actin as shown by counterstaining with fluores-

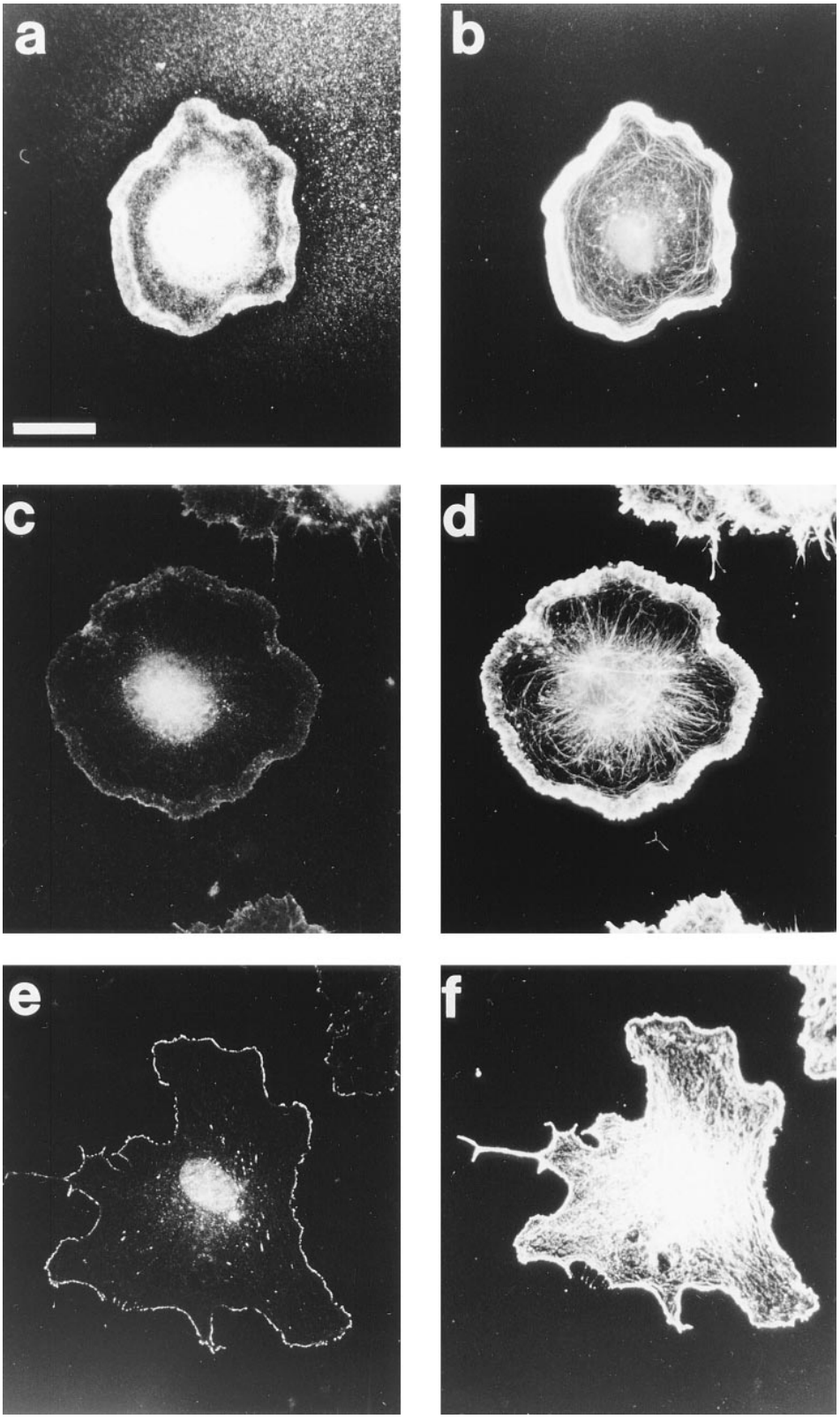

Figure 9. Response of cells plated on poly-L-lysine to Rac activation. Serum-starved quiescent Swiss 3T3 cells were trypsinized and plated onto poly-L-lysine (10 μg/ml)–coated coverslips for 20 min (*a–d*) or fibronectin-coated coverslips for 2 h (*e* and *f*). (*a*) Cy3-actin fluorescence in a cell 20 min after comicroinjection of Cy3-actin and L61 Rac protein. (*b*) Counterstain of the same cell with fluorescein phalloidin. (*c*) The distribution of vinculin in a cell treated for 20 min with PDGF and counterstained with rhodamine phalloidin (*d*). (*e*) Vinculin in normal focal complexes formed after PDGF treatment for 20 min. (*f*) Rhodamine phalloidin counterstain of the same cell. Bar, 5 μm.

cein phalloidin (Fig. 9 *b*). These lamellipodia appear enriched in vinculin (Fig. 9 *c*; same cell counterstained with rhodamine phalloidin, Fig. 9 *d*), but they have no detectable organized focal complexes like those seen on fibronectin (Fig. 9 *e*; same cell counterstained with rhodamine phalloidin, Fig. 9 *f*) (20). Rac- and PDGF-induced lamellipodia in cells plated on poly-L-lysine also appear wider in proportion to the cell body size and more uniform around

the periphery of the cell than lamellipodia induced in cells plated on fibronectin (Fig. 9 *f*). Using video microscopy, we found that the cells retained the ability to ruffle on poly-L-lysine in a manner largely indistinguishable from cells on fibronectin-coated surfaces (not shown). Cells plated on Con A–coated coverslips also extend lamellipodia in response to microinjection of activated Rac protein, and ruffles can be observed by time-lapse video that are indistinguishable from those formed on fibronectin substrates (not shown). Thus Rac-induced focal complexes are not important for lamellipodium extension, ruffling, or actin polymerization in the lamellipodium.

Discussion

Rac and Rho Activation Mobilize Different Pools of Actin in the Cell

Despite the widespread assumption that Rac and Rho induce actin polymerization when activated, this is to our knowledge the first quantitative study of F-actin levels in fibroblasts in response to activation of Rac and Rho. Our results show that activation of endogenous Rac (by PDGF) transiently increases F-actin by ~30%; this is reflected in the transient nature of the ruffling response induced by PDGF (Fig. 1). In contrast, the transient increase in F-actin in cells treated with sphingosine-1-p was not reflected by a decrease in stress fibers. Our Cy3-actin results suggest that new F-actin must be diffuse in cells during stress fiber formation and we favor the explanation that the F-actin increase may be due to a stabilization of F-actin brought about by bundling rather than a burst of actin polymerization. Simultaneous activation of Rac and Rho produced a larger (40%) and more sustained increase in F-actin. This may be due to an additive effect of Rac and Rho mobilizing distinct pools of F-actin in cells, or could alternatively be due to a combinatorial effect such as Rac inducing actin polymerization and Rho inducing stability by reducing turnover rates.

Stress Fibers Assemble by Bundling Existing F-actin and Concomitant Integrin Clustering

We have found that de novo stress fiber formation as a result of activation of Rho occurs by the merging of smaller disorganized F-actin bundles. Using Cy3-actin as a probe, we did not observe any localized actin polymerization during stress fiber formation. This was somewhat surprising in light of suggestions that Rho can activate a PI 4P 5-kinase and stimulate actin polymerization in a similar way as that proposed for Rac (6). Previous studies indicate, however, that Rho activation does not enhance cell motility, and can even retard it (26), a finding which agrees with the lack of a need for a burst of directional actin polymerization. In addition, ADP-ribosylation of Rho with C3 transferase does not reduce the actin polymerization response of neutrophils to f-Met-Leu-Phe and may even increase it (8, 17), perhaps because Rho normally maintains stable actin filament assemblies not used in cell motility.

The mechanism by which Rho mediates actin filament bundling may include the Rho-binding serine/threonine kinase p160 Rho-kinase, which phosphorylates the myosin-binding subunit of myosin light chain phosphatase (16) and thus may promote assembly and contractility of stress fibers. Recent studies have shown that p160 Rho-kinase activation itself promotes stress fiber and focal adhesion assembly (18), so it may be that actin filaments are stabilized by assembly of acto-myosin contractile bundles rather than that any direct induction of actin polymerization occurs with Rho activation.

Rho Induces Actin-Myosin Bundles and Vinculin-Actin Association in the Absence of Integrin Clustering

This laboratory previously reported that activation of Rho in cells plated on poly-L-lysine led to the assembly of disorganized actin filament bundles. In that report we speculated that Rho was inducing actin polymerization independently of integrin clustering (13). We now report that myosin and vinculin localize along these bundles and that they appear to be contractile. Cy3-actin microinjection suggests that these structures are formed from bundling of preexisting actin filaments, which are diffuse and below the level of resolution of the microscope, in starved cells. Both myosin and vinculin may play an active role in stabilizing and bundling the actin filaments. This raises the interesting possibility that Rho activation might stimulate an association of vinculin with actin or actin-binding proteins that is independent of integrin clustering in focal adhesions. Gilmore at al. (9) have demonstrated a phosphoinositide-regulatable actin-binding site on vinculin, and one possibility is that Rho may promote vinculin-actin association by stimulation of PI 4P 5-kinase even under conditions where integrin clustering is prevented. This association of vinculin along F-actin bundles may have an active role in assembly and maintenance of both stress fibers and focal adhesions. Support for this idea comes from studies on vinculin null cells, where focal adhesions and stress fibers are absent and integrins and talin localize in patches under the plasma membrane, while paxillin is diffuse in the cytoplasm (10). We cannot rule out that our vinculin-actin association may be mediated by some aberrant association between integrins and poly-L-lysine, but since the interaction is EDTA-insensitive, and we only see these clusters after Rho activation, we think that this is unlikely. This result is somewhat different from a previous report from this laboratory showing that vinculin was diffuse in cells plated on poly-L-lysine (13). This discrepancy is due to a triple labeling technique used in our current study with fluoresceinated secondary and tertiary antibodies, which allowed a more sensitive resolution of vinculin clusters.

Rac-induced Lamellipodia Contain Polymerizing Actin and Are Formed Independently of Integrin-mediated Adhesion

By time-lapse video microscopy, the peripheral regions of cells microinjected with constitutively active Rac show immediate lamellipodium extension and ruffling, and coinjection of Cy3-actin shows that the lamellipodium is rich in polymerizing actin. Our observations in intact cells agree with the work of Hartwig et al. who used permeabilized human platelets to show that Rac induces an actin polymerization signal at the cell periphery (12). It is not surprising that cells that are extending fresh lamellipodia are polymeriz-

ing actin; this has been shown in motile cells using labeled actin and also photobleaching (7, 28, 32, 33). It is perhaps more surprising that, in cells which are starved for serum, actin polymerization is not observed in the periphery of the cell, while it is observed within 5 min after injection of Rac. This suggests that the cell periphery contains a combination of capped actin filaments and the machinery to cause a rapid burst of actin polymerization. Furthermore, this machinery is tightly controlled so that, analogously to platelet activation by thrombin, actin polymerization is triggered in response to a signal to extend a lamellipodium. This response seems to be immediate (within 5 min) and constant in magnitude over a short time course (20 min), but it may be variable with the amount of activated Rac, as microinjection of constitutively active Rac produced a consistently larger response than did PDGF treatment.

In cells plated on fibronectin, Rac activation induces the formation of peripheral focal complexes containing focal adhesion proteins (20). Cells plated on poly-L-lysine or Con A are unable to form focal complexes in response to Rac activation, but are still able to extend lamellipodia that contain normal levels of polymerized Cy3-actin. There is a low level of diffuse vinculin staining in the lamellipodia of these cells, which colocalizes with the actin staining, suggesting that vinculin may be associated with the lamellar actin even in the absence of focal complexes. It is clear from these observations that focal complexes are not sites of actin polymerization, nor are they required for the lamellipodium to extend. Rac-induced lamellipodia do have a different morphology on poly-L-lysine than on fibronectin; they are wider and run continuously around the periphery of the cell. Integrin clustering thus seems to be required for spatial regulation of lamellipodium extension and perhaps for stabilization of the lamellipodium in cell motility.

In summary, we have shown that actin polymerizes in peripheral regions during Rac-induced lamellipodium extension in fibroblasts, but that Rho-induced stress fiber formation occurs through the bundling of actin filaments. Focal adhesions are not sites of enhanced actin polymerization in cells during stress fiber assembly, and focal complexes are not required for lamellar actin assembly.

We thank Drs. J.V. Small and K. Rottner for sharing unpublished results and for bringing to our attention the rings of actin filaments in starved cells. We thank Dr. Sally Zigmond for helpful discussions in the early stages of this work. We also thank David Drechsel and Robert Insall for critical reading of the manuscript and Tina Bridges for preparing the recombinant Rac and Rho proteins.

This work is supported in part by the Damon Runyon-Walter Winchell Cancer Research Fund, The Cancer Research Campaign (CRC), and the Medical Research Council (MRC). L. Machesky currently holds an MRC Career Development Award.

Received for publication 11 December 1996 and in revised form 21 May 1997.

References

1. Bershadsky, A., A. Chausovsky, E. Becker, A. Lyubimova, and B. Geiger. 1996. Involvement of microtubules in the control of adhesion-dependent signal transduction. *Curr. Biol.* 6:1279–1289.
2. Bretcher, M.S. 1996. Getting membrane flow and the cytoskeleton to cooperate in moving cells. *Cell.* 87:601–606.
3. Burridge, K., and K. Fath. 1989. Focal contacts: transmembrane links between the extracellular matrix and the cytoskeleton. *Bioessays.* 10:104–108.
4. Burridge, K., K. Fath, T. Kelly, G. Nuckolls, and C. Turner. 1988. Focal Adhesions: transmembrane junctions between the extracellular matrix and the cytoskeleton. *Annu. Rev. Cell Biol.* 4:487–525.
5. Burridge, K., G. Nuckolls, C. Otey, F. Pavalko, K. Simon, and C. Turner. 1990. Actin membrane interaction in focal adhesions. *Cell Differ. Dev.* 32:337–342.

5a. Carson, M., A. Weber, and S.H. Zigmond. 1986. An actin-nucleating activity in polymorphonuclear leukocytes is modulated by chemotactic peptides. *J. Cell Biol.* 103:2707–2714.

6. Chong, L.D., A. Traynor-Kaplan, G.M. Bokoch, and M.A. Schwartz. 1994. The small GTP-binding protein Rho regulates a phosphatidylinositol 4-phosphate 5-kinase in mammalian cells. *Cell.* 79:507–513.
7. Debiasio, R.L., L.-L. Wang, G.W. Fisher, and D.L. Taylor. 1988. The dynamic distribution of fluorescent analogs of actin and myosin in protrusions at the leading edge of migrating Swiss 3T3 fibroblasts. *J. Cell Biol.* 107:2631–2645.
8. Ehrengruber, M.U., P. Boquet, T.D. Coates, and D.A. Deranleau. 1995. ADP-ribosylation of Rho enhances actin polymerization-coupled shape oscillations in human neutrophils. *FEBS Lett.* 372:161–164.
9. Gilmore, A.P., and K. Burridge. 1996. Regulation of vinculin binding to talin and actin by phosphatidyl-inositol-4-5-bisphosphate. *Nature (Lond.).* 381:531–535.
10. Goldmann, W.H., M. Schindl, T.J. Cardozo, and R.M. Ezzell. 1995. Motility of vinculin-deficient F9 embryonic carcinoma cells analyzed by video, laser confocal, and reflection interference contrast microscopy. *Exp. Cell Res.* 221:311–319.
11. Hall, A.L., V. Warren, S. Dharmawardhane, and J. Condeelis. 1989. Identification of actin nucleation activity and polymerization inhibitor in ameboid cells: their regulation by chemotactic stimulation. *J. Cell Biol.* 109: 2207–2213.
12. Hartwig, J.H., G.M. Bokoch, C.L. Carpenter, P.A. Janmey, L.A. Taylor, A. Toker, and T.P. Stossel. 1995. Thrombin receptor ligation and activated Rac uncap actin filament barbed ends through phosphoinositide synthesis in permeabilized human platelets. *Cell.* 82:643–653.
13. Hotchin, N.A., and A. Hall. 1995. The assembly of integrin complexes requires both extracellular matrix and intracellular rho/rac GTPases. *J. Cell Biol.* 131:1857–1865.
14. Howard, T.H., and W.H. Meyer. 1984. Chemotactic peptide modulation of actin assembly and locomotion in neutrophils. *J. Cell Biol.* 98:1265–1271.
15. Howard, T.H., and D. Wang. 1987. Calcium ionophore, phorbol ester, and chemotactic peptide-induced cytoskeleton reorganization in human neutrophils. *J. Clin. Invest.* 79:1359–1364.
16. Kimura, K., M. Ito, M. Amano, K. Chihara, Y. Fukata, M. Nakafuku, B. Yamamori, J.H. Feng, T. Nakano, K. Okawa et al. 1996. Regulation of myosin phosphatase by Rho and Rho-associated kinase (Rho-kinase). *Science (Wash. DC).* 273:245–248.
17. Koch, G., J. Norgauer, and K. Aktories. 1994. ADP-ribosylation of the GTP-binding protein Rho by Clostridium linosum exoenzyme affects basal, but not N-formyl-peptide-stimulated, actin polymerization in human myeloid leukaemic (HL60) cells. *Biochem. J.* 299:775–779.
18. Leung, T., X.Q. Chen, E. Manser, and L. Lim. 1996. The p160 RhoA-binding kinase ROK α is a member of a kinase family and is involved in the reorganization of the cytoskeleton. *Mol. Cell. Biol.* 16:5313–5327.
19. Martenson, C., K. Stone, M. Reedy, and M. Sheetz. 1993. Fast axonal transport is required for growth cone advance. *Nature (Lond.).* 366:66–69.
20. Nobes, C.D., and A. Hall. 1995. Rho, rac and cdc42 regulate the assembly of multi-molecular focal complexes associated with actin stress fibers, lamellipodia and filopodia. *Cell.* 81:53–62.
21. Pollard, T.D., and J.A. Cooper. 1984. Quantitative analysis of the effect of acanthamoeba profilin on actin filament nucleation and elongation. *Biochemistry.* 23:6631–6641.
22. Postma, F.R., K. Jalink, T. Hengeveld, and W.H. Moolenaar. 1996. Sphingosine-1-phosphate rapidly induces Rho-dependent neurite retraction: action through a specific cell surface receptor. *EMBO (Eur. Mol. Biol. Organ.) J.* 15:2388–2392.
23. Ren, X.D., G.M. Bokoch, A. Traynorkaplan, G.H. Jenkins, R.A. Anderson, and M.A. Schwartz. 1996. Physical association of the small GTPase Rho with a 68-kDa phosphatidylinositol 4-phosphate 5-kinase in Swiss 3T3 cells. *Mol. Biol. Cell.* 7:435–442.
24. Ridley, A.J., and A. Hall. 1992. The small GTP-binding protein Rho regulates the assembly of focal adhesions and actin stress fibers in response to growth factors. *Cell.* 70:389–399.
25. Ridley, A.J., H.F. Paterson, C.L. Johnston, D. Diekmann, and A. Hall. 1992. The small GTP-binding protein Rac regulates growth factor induced membrane ruffling. *Cell.* 70:401–410.
26. Ridley, A.J., P.M. Comoglio, and A. Hall. 1995. Regulation of scatter factor hepatocyte growth factor responses by Ras, Rac, and Rho in MDCK cells. *Mol. Cell. Biol.* 15:1110–1122.
27. Sanders, M.C., and Y.-L. Wang. 1990. Exogenous nucleation sites fail to induce detectable polymerization of actin in living cells. *J. Cell Biol.* 110:359–365.
28. Simon, J.R., A. Gough, E. Urbanik, F. Wang, F. Lanni, B.R. Ware, and D.L. Taylor. 1988. Analysis of rhodamine and fluorescein-labeled F-actin diffusion in vitro by fluorescence photobleaching recovery. *Biophys. J.* 54:801–815.
29. Spudich, J.A., and S. Watt. 1971. The regulation of rabbit skeletal muscle contraction. I. Biochemical studies of the interaction of the tropomyosin-troponin complex with actin and the protein fragments of myosin. *J. Biol. Chem.* 246:4866.

30. Stossel, T.P. 1993. On the crawling of animal cells. *Science (Wash. DC).* 260:1086–1094.
31. Symons, M.H., and T.J. Mitchison. 1991. Control of actin polymerization in live and permeabilized fibroblasts. *J. Cell Biol.* 114:503–513.
32. Wang, Y.-L. 1985. Exchange of actin subunits at the leading edge of living fibroblasts: possible role of treadmilling. *J. Cell Biol.* 101:597–602.
33. Wang, Y.-L. 1984. Reorganization of actin filament bundles in living fibroblasts. *J. Cell. Biol.* 99:1478–1485.
34. Wegner, A., and J. Engel. 1975. Kinetics of the cooperative association of actin to actin filaments. *Biophys. Chem.* 3:215–225.
35. Yamada, K., and S. Miyamoto. 1995. Integrin transmembrane signaling and cytoskeletal control. *Curr. Opin. Cell Biol.* 7:681–689.
36. Zigmond, S.H. 1996. Signal transduction and actin filament organization. *Curr. Opin. Cell Biol.* 8:66–73.